Recurrence condensation during critical transitions in complex systems

Manaswini Jella, Induja Pavithran, Vishnu R. Unni, Norbert Marwan, Jürgen Kurths, R.I. Sujith

Originally published as
Jella, M., Pavithran, I., Unni, V.R., Marwan, N., Kurths, J., Sujith, R.I. (2025): Recurrence condensation during critical transitions in complex systems. - Chaos, 36, 8, 083107.
https://doi.org/10.1063/5.0267157

RESEARCH ARTICLE | AUGUST 01 2025

Recurrence condensation during critical transitions in complex systems

Manaswini Jella ; Induja Pavithran ; Vishnu R. Unni ; Norbert Marwan ; Jürgen Kurths ; R. I. Sujith

Chaos 35, 083107 (2025)
https://doi.org/10.1063/5.0267157

Chaos ARTICLE pubs.aip.org/aip/cha

Recurrence condensation during critical transitions in complex systems

Cite as: Chaos 35, 083107 (2025); doi: 10.1063/5.0267157
Submitted: 22 February 2025 · Accepted: 15 July 2025 ·
Published Online: 1 August 2025

View Online Export Citation CrossMark

Manaswini Jella,[1,2] Induja Pavithran,[2,3,a)] Vishnu R. Unni,[4] Norbert Marwan,[5,6] Jürgen Kurths,[5,7] and R. I. Sujith[2,3]

AFFILIATIONS

[1] Department of Mechanical Engineering, Indian Institute of Technology Madras, Chennai 600036, India
[2] Centre of Excellence for Studying Critical Transitions in Complex Systems, Indian Institute of Technology Madras, Chennai 600036, India
[3] Department of Aerospace Engineering, Indian Institute of Technology Madras, Chennai 600036, India
[4] Department of Mechanical and Aerospace Engineering, Indian Institute of Technology Hyderabad, Kandi, Telangana 502284, India
[5] Potsdam Institute for Climate Impact Research (PIK), Member of the Leibniz Association, Potsdam 14412, Germany
[6] Institute for Physics and Astronomy, University of Potsdam, Potsdam 14476, Germany
[7] Department of Physics, Humboldt Universität zu Berlin, Berlin 10117, Germany

[a)] **Author to whom correspondence should be addressed:** indujap2013@gmail.com. **Present address:** Jacob Blaustein Institute for Desert Research, Ben-Gurion University of the Negev, Midreshet Ben-Gurion 8499000, Israel.

ABSTRACT

Critical transitions in complex systems pose challenges for the healthy functioning of natural and engineered systems, sometimes with catastrophic outcomes. These critical points, where small changes cause large regime shifts, are difficult to detect—especially in noisy, high-dimensional settings. We investigate such a transition from chaotic to periodic oscillations via intermittency in a turbulent fluid mechanical system by using recurrence analysis. Recurrence plots (RPs) constructed from the time series of a state variable reveal a distinct progression from disordered, short broken diagonal lines to patches of ordered short diagonal lines and, ultimately, to a pattern of long continuous diagonal lines. This evolution in the recurrence patterns captures a transition from dynamics involving multiple time scales to a dominant single time scale; we term this phenomenon "recurrence condensation." We quantify recurrence condensation using recurrence quantification measures, such as the recurrence time, determinism, entropy, laminarity, and trapping time, all of which show collapse to a single dominant time scale. Furthermore, these recurrence measures exhibit power-law scaling with the deviation of the control parameter from the critical point. Optimizing for the best power law reveals the critical value of the parameter. We apply this method to the synthetic data from a basic noisy Hopf bifurcation model and confirm that the detected critical point coincides with the bifurcation point. Our findings offer insights into identifying the critical points in noisy systems with gradual transitions, where the transition point is not well defined.

Critical transitions marked by sudden shifts in the dynamical behavior of complex systems are a subject of study across disciplines, including climate science, ecology, biology, and engineering. These shifts can lead to catastrophic outcomes, making their early detection crucial. Traditional methods for identifying the critical points in nonlinear systems rely on statistical techniques, but their effectiveness diminishes due to the limited availability of long time series, the presence of noise, and the gradual nature of transitions. Recent advancements in recurrence analysis provide a powerful framework for capturing subtle dynamical changes. In this study, we use recurrence plots (RPs) to investigate the transition from chaotic to periodic oscillations in a turbulent fluid system. We introduce the concept of recurrence condensation, wherein recurrence patterns evolve from disordered to highly ordered structures as the system approaches periodicity. By quantifying this phenomenon using recurrence measures, such as recurrence time, determinism, entropy, laminarity, and trapping time, we uncover a power-law scaling behavior as we approach the critical point. Additionally, application of this method to a noisy Hopf bifurcation model confirms its ability

to detect the critical transition point consistent with the bifurcation point. These findings support the use of recurrence analysis to identify the critical points in noisy, high-dimensional systems, thereby also helping to develop effective early warning signals (EWSs) for impending tipping points in real-world systems.

I. INTRODUCTION

Complex systems comprise interconnected networks of components or subsystems, whose nonlinear interactions give rise to intricate dynamic behavior.[1] Key characteristics of a complex system include nonlinearity, spontaneous emergence of order, adaptation, and feedback loops.[2] Understanding these complex systems is essential for addressing real-world challenges with applications in diverse fields such as ecology,[3] financial markets,[4,5] climate,[6] and biology.[7,8]

Complex systems often exhibit multi-stability, making them prone to sudden and unexpected shifts from one state to another. Such transitions are referred to as critical transitions.[9] These transitions may arise from a bifurcation due to slowly varying parameters, or from perturbations that push the system beyond a stability threshold, or from a rapid change in a parameter. In the regime of multi-stability, sufficiently high perturbations can abruptly shift the system into a new dynamical state. Comprehending and anticipating such critical transitions are important, as they are associated with several high-stakes scenarios, such as ecosystem collapses,[10] climate regime shifts,[11] financial market crashes,[12] failures in engineering systems,[13,14] and the progression of infectious diseases.[15]

Critical transitions in fluid mechanical systems—such as thermoacoustic, aeroacoustic, and aeroelastic systems—often manifest as transitions from small-amplitude aperiodic oscillations to high-amplitude oscillatory instabilities,[16] driven by positive feedback mechanisms. In aeroacoustic systems such as flutes[17] and large segmented solid rocket motors,[18] feedback arises from the interaction between the acoustic field and the vortex shedding in closed confinements. In thermoacoustic systems, the feedback is between the acoustic field and the unsteady heat release rate. In engineering parlance, the terms combustion noise and thermoacoustic instability refer to low-amplitude chaotic fluctuations and high-amplitude self-sustained periodic oscillations in acoustic pressure, respectively.[19] These large amplitude acoustic pressure oscillations during thermoacoustic instabilities pose significant threats to the overall health and functionality of systems such as rockets and gas turbine engines. These oscillations can lead to increased heat transfer that overwhelms the thermal protection systems, failures in guidance, navigation, and control systems, and damage to electronic components and payloads. These sudden transitions can lead to catastrophic outcomes, compromising the safety and structural integrity of the systems.[19,20] These transitions reflect the emergence of order from disorder through self-organization, where coherent spatiotemporal patterns emerge from the initially disordered states due to positive feedback.[21]

Well-known examples of self-organization include the Rayleigh–Benard convection,[22] where increasing the temperature gradient leads to a shift from the uncoordinated movements of fluid particles to an ordered rolling motion. Here, specific oscillatory modes begin to dominate, giving rise to coherent spatiotemporal patterns. Similarly, the Ising model describes a phase transition from a state of disordered spins to an ordered long range magnetic order at a critical temperature known as the Curie temperature.[23] In biological systems, Turing patterns provide a mathematical framework for understanding how complex, self-organized, repeating patterns can emerge from reaction-diffusion systems.[24]

Bose–Einstein condensation in quantum systems is another phenomenon demonstrating self-organization, where particles collectively occupy the same low-energy quantum state and behave like a wave, creating an organized pattern near absolute zero.[25] Analogous condensation phenomena have been observed in classical systems—for example, during laser light condensation[26] and thermoacoustic instability.[27] During the transition to thermoacoustic instability, the phase space topology consisting of several unstable periodic orbits condenses into a stable periodic orbit.[27] These phenomena illustrate how ordered states emerge naturally from the initially disordered states.[28–31]

Self-organization leading to oscillatory instabilities in fluid mechanical systems has been described as spectral condensation,[32] where the energy distributed in a broadband of frequencies converges to a dominant mode of oscillations. Spectral condensation has been studied elaborately in fluid mechanical, electronic, and optical systems.[32] This transition is captured by spectral measures following an inverse power-law behavior with the power of the dominant mode in the power spectrum.[32] Recurrence plots (RPs) and Recurrence quantification analysis (RQA)[33] offer powerful tools to study such dynamical transitions. RPs are useful for visually representing multidimensional phase space in a concise, two-dimensional format, highlighting various recurrence patterns. RQA quantifies the patterns present in the RP using measures based on the density of the recurrence points, and also the diagonal and the vertical line structures. RQA is used successfully in describing various dynamical states such as periodicity, chaos, and other states.[34,35] Moreover, measures derived from the RPs have been employed to detect transitions[7,11,36,37] and serve as early warning signals for impending transitions.[35,38,39]

Considering the broad applicability and advantages of RQA, we apply it to investigate the critical transition to oscillatory instability in a turbulent thermoacoustic system. The thermoacoustic system was chosen for this study due to its practical relevance and rich nonlinear dynamics. This system exhibits a transition from chaotic fluctuations to periodic oscillations—an example of self-organization in high-dimensional nonlinear systems. As these transitions can lead to structural or operational failures in systems such as gas turbines and rockets, early detection is crucial. Recurrence-based methods are well-suited for this problem, given the noisy and short-duration nature of the experimental data. As the Reynolds number (*Re*) is varied, the system undergoes a transition from low-amplitude chaotic fluctuations to high-amplitude self-sustained periodic oscillations via intermittency.[40] RPs have previously been used to study intermittency, flame blowout, and also to understand the transition from combustion noise to thermoacoustic instability.[41,42] In this work, we investigate the transformation in the patterns of the RPs during critical transitions from a chaotic state to thermoacoustic instability, i.e., the transition from a disordered arrangement of short, broken diagonal lines to a pattern of long, continuous diagonal lines. As the length of a diagonal line is determined by the duration of a similar evolution in trajectory segments,[35] the transition from combustion noise (chaotic) to thermoacoustic instability (periodic) can be viewed as a condensation from multiple recurrence time scales to a single dominant time scale; we refer to this phenomenon as recurrence condensation. This transition from a chaotic state to a periodic state exhibits features of self-organization, similar to those observed during spectral condensation.[32] We quantify recurrence condensation using RQA measures and calculate the recurrence times to demonstrate the condensation from multiple peaks to a single dominant peak in the spectrum of recurrence times.

In physics, condensation and critical transitions are often studied in the framework of phase transitions, where scaling laws are typically defined in terms of the deviation from the critical transition point.[43] The study by Afsar *et al.*[44] illustrated an interesting application of recurrence quantification analysis (RQA) in the context of the critical transitions in dynamical systems, particularly in period-doubling bifurcations. The discovery that RQA measures follow power laws has significant implications for understanding the critical transitions in fluid mechanical systems. Inspired by their work, we employ RPs and RQA to explore the transitions in thermofluid systems to identify power-law scaling. Our results show that determining such power laws can serve as a powerful tool in identifying the critical points within noisy systems undergoing gradual transitions—especially in cases where conventional definitions of the critical points are ambiguous.

II. METHODS

A. Experimental setup

We conduct experiments in a turbulent combustor, having a backward facing step and a circular bluff body to stabilize the flame. A schematic of the experimental setup is shown in Fig. 1. Compressed air enters the plenum chamber, where it mixes with the fuel, before entering the combustion chamber, where a spark plug powered by an 11 kV transformer ignites the combustible mixture. The fuel entering the combustion chamber is liquid petroleum gas (LPG), comprising 60% propane and 40% butane by volume.

We use a constant fuel flow rate of 28 SLPM and quasi-statically vary the air flow rate from 410 to 650 SLPM in steps of 10 SLPM. The mass flow rates of both fuel and air are measured using mass flow controllers (Alicat Scientific, MCR Series) with an uncertainty of $\pm 0.8\%$ of the reading $\pm 0.2\%$ of the full scale. The bluff body is positioned 45 mm downstream of the dump plane and has a diameter of 47 mm and a thickness of 10 mm. The acoustic pressure fluctuations are measured using a piezoelectric pressure transducer PCB103B02 (resolution of 0.15 Pa) at a sampling frequency of 10 kHz for 3 s. A 16-bit analog to digital converter (NI-6143) is used for data acquisition.

As the air flow rate is increased, Re increases accordingly. Re is calculated as $Re = 4\dot{m}D_1/\pi\mu D_0^2$, where the hydraulic diameter of the burner (D_0) is 40 mm, the diameter of the bluff body (D_1) is 47 mm, $\dot{m}$ and μ are the total flow rate and the coefficient of dynamic viscosity of the fuel–air mixture entering the combustion chamber, respectively. We use the dynamic viscosity equation as stated by Wilke[45] to calculate the Reynolds number. As the Reynolds number is varied from $(2.13 \pm 0.066) \times 10^4$ to $(3.18 \pm 0.072) \times 10^4$, the pressure fluctuations change from chaos to limit cycle oscillations (LCO). Here, LCO corresponds to the self-sustained periodic oscillations during thermoacoustic instability. A detailed description of the experimental setup and the measurements are provided in Nair and Sujith.[40]

B. Noisy Hopf bifurcation model

We examine a nonlinear self-excited oscillator model in the presence of noise, which exhibits both subcritical and supercritical Hopf bifurcations. Following Noiray *et al.*,[46] we include additive white noise ξ of intensity Γ and having an autocorrelation $\langle \xi\xi_\tau \rangle = \Gamma\delta(\tau)$,

$$\ddot{\eta} + \alpha\dot{\eta} + \omega^2\eta = \dot{\eta}(\beta + K\eta^2 - \gamma\eta^4) + \xi. \quad (1)$$

The parameters $\omega = 2\pi \times 120$ rad/s, $\beta = 50$ rad/s, $\gamma = 0.7$, $K = 9$, and $\Gamma = 10$ are kept constant. Following Pavithran *et al.*,[32] these parameter values are selected to capture the transition from low-amplitude aperiodic fluctuations to high-amplitude limit cycle

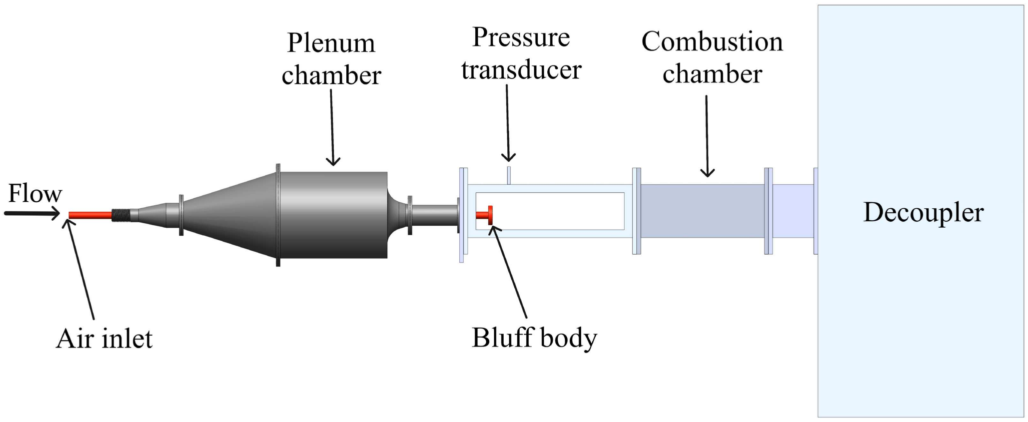

FIG. 1. Schematic of the turbulent combustor used in this study. The pressure transducer mounted on the combustion chamber measures the acoustic pressure fluctuations.

oscillations via a subcritical Hopf bifurcation. For obtaining a supercritical Hopf bifurcation, we choose $\gamma = -0.7$ and $K = -9$. The time series of η is acquired across a range of linear damping term (α) values. Specifically, α is varied from 80 to 45 rad/s to capture the subcritical and supercritical Hopf bifurcations.

C. Recurrence plot construction

Recurrence is a fundamental property of deterministic dynamical systems, and identifying the underlying recurrence patterns enables us to understand the various dynamical states during a transition. RPs were first introduced by Eckmann *et al.*[47] They allow us to visualize the time instants when the trajectory of the measured time signal visits roughly the same area in the phase space. A point in the phase space is considered recurrent if the phase space trajectory revisits the close neighborhood of its previous location at a particular time lag. If not all state variables of the system are available, we can reconstruct a hypothetical phase space from the measured time series. This phase space reconstruction is achieved by creating delay vectors derived from the single measured time series. The phase portrait of the given dynamical system is constructed in an appropriate low-dimensional phase space using Takens' delay embedding theorem. For a time series $x(t_i)$, $i = 1, 2, \ldots, N$, the embedding dimension m is calculated using Cao's algorithm,[48] and the average mutual information method[49] is used to find the optimum time delay τ. The delay vectors generated are given by $\vec{X}(t_i) = x(i), x(i+\tau), \ldots, x(i+(m-1)\tau)$.

A phase space vector $\vec{X}$ is said to be recurrent if the pairwise distance between $\vec{X}(t_i)$ and $\vec{X}(t_j)$ is less than the recurrence threshold ε. The resulting recurrence matrix $\mathbf{R}$ is binary, consisting of zeros and ones, where ones indicate the points in phase space that recur after a certain time lag, and zeros indicate nonrecurrent state points,[33]

$$R_{i,j} = \Theta(\varepsilon - \|\vec{X}(t_i) - \vec{X}(t_j)\|). \tag{2}$$

Here, Θ is the Heaviside function and $\|\cdot\|$ represents the Euclidean norm. In this study, we represent the value 1 in the matrix $\mathbf{R}$ using black color, and, for simplicity, refer to recurrence points $R_{i,j} = 1$ as "black points" and non-recurrence points $R_{i,j} = 0$ as "white points." Here, ε is a threshold to define the neighborhood of a state point in the reconstructed phase space. ε can be selected using different approaches[50] depending on the information we plan to extract from recurrence analysis.

Choosing the recurrence threshold ε is important for meaningful RPs and RQA. A fixed ε is appropriate when comparing the data with similar scales or when the absolute values are meaningful.[50] However, for experimental data where amplitudes can fluctuate, an adaptive threshold can be used. One common approach is to fix the recurrence rate $RR(\varepsilon) = \sum_{i,j}^{N} R_{i,j}(\varepsilon)/N^2$ by adjusting ε, which effectively serves as an adaptive threshold. This helps to maintain a constant density of recurrence points and enables consistent comparisons across datasets.[51] In this study, we use both fixed and adaptive ε thresholds. A fixed ε is used to clearly visualize the RPs and to capture the multiple time scales present. For RQA, we fix the RR at 0.05 to enable consistent comparison of measures across states; this ensures that the recurrence points represent the smallest 5% of pairwise distances in the phase space.

D. Recurrence quantification measures

The information contained in an RP can be quantified using recurrence point density, as well as diagonal and vertical line structures. The methods based on diagonal and vertical lines rely on the histogram of their corresponding lines.[35]

The recurrence rate (RR) quantifies the density of recurrence points within a recurrence matrix $\mathbf{R}$, representing the percentage of recurrence in the phase space,

$$RR = \frac{1}{N^2} \sum_{i,j}^{N} R_{i,j}. \tag{3}$$

τ recurrence rate (τ-RR) quantifies the density of recurrence points along a diagonal line in the recurrence matrix. These diagonal lines are at a distance of τ units perpendicular to the main diagonal line,[52]

$$\tau\text{-RR} = \frac{1}{N-\tau} \sum_{i}^{N-\tau} R_{i,i+\tau}. \tag{4}$$

Since τ-RR measures the recurrence rate along a diagonal line, those RPs with long, continuous diagonal lines have a higher τ-RR. This is because long diagonal lines indicate sustained recurrence over time. Conversely, the RPs characterized by broken diagonal lines will result in a lower τ-RR. The τ-RR typically exhibits a spike-train-like structure, where spikes correspond to high recurrence rates at specific lags. This structure reflects the underlying periodicities or patterns in the time series. To analyze these periodicities effectively, the inter-spike spectrum (ISS) serves as an effective tool (refer Appendix).

1. Measures based on diagonal lines

Measures based on the length of the diagonal lines depend on the likelihood of finding a diagonal line of length (l) in the RPs. The diagonal line in a recurrence plot is closely related to the duration of a similar evolution in a trajectory. By optimally setting the minimal diagonal length ($l_{\min}$), it is possible to exclude diagonal lines that are formed by tangential motion rather than similar evolution.

Determinism (DET) is the ratio of recurrence points that form diagonal lines of length l greater than the minimum length of $l_{\min}$ to the total number of recurrence points in R,

$$DET = \frac{\sum_{l=l_{\min}}^{N} lP(l)}{\sum_{l=1}^{N} lP(l)}. \tag{5}$$

DET often reflects the predictability of the system.[53] Due to the presence of longer diagonal lines, the value of DET is generally higher for deterministic processes than stochastic processes.

The average diagonal line length (L) measures the average time that two segments of the trajectory are in a close neighborhood. This measure can be interpreted as the average prediction time, as it reflects how long the system is likely to evolve in a manner similar to the evolution of another state,

$$L = \frac{\sum_{l=l_{\min}}^{N} lP(l)}{\sum_{l=l_{\min}}^{N} P(l)}. \tag{6}$$

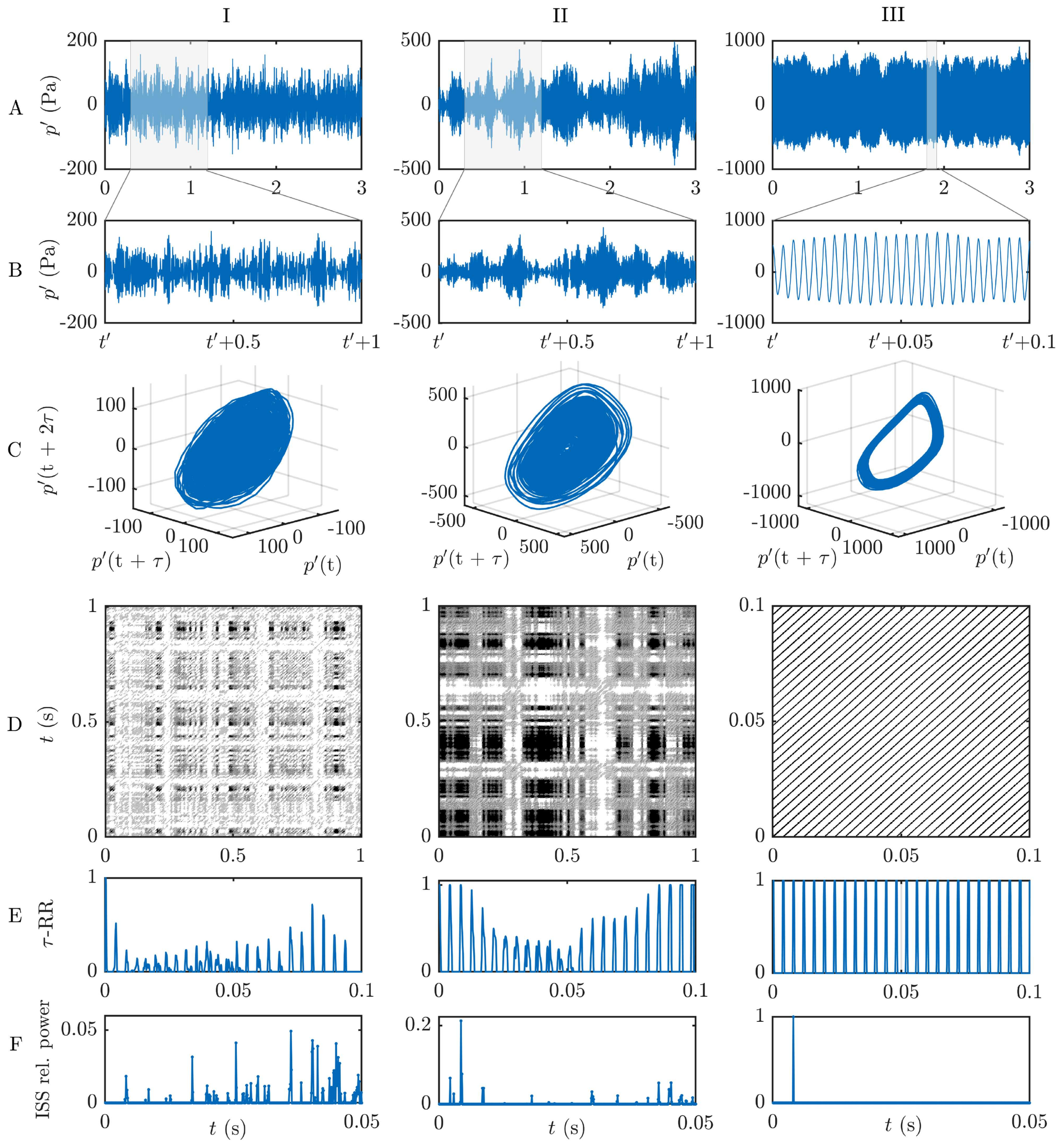

FIG. 2. Visualizing recurrence condensation using the τ-recurrence rate and the inter-spike spectrum. The time series of acoustic pressure fluctuations in a bluff body stabilized combustor during the state of combustion noise I-(A) (chaotic regime at $Re = 2.13 \times 10^4$), intermittency II-(A) ($Re = 2.88 \times 10^4$), and thermoacoustic instability III-(A) (LCO at $Re = 3.09 \times 10^4$). The corresponding phase portraits illustrate the evolution of the attractor across these regimes (I–III)(C). RPs (D) were constructed for a time series window of 1, 1, and 0.1 s (B), respectively, using a recurrence threshold corresponding to 20% of the attractor size. (I)–(III)(E) τ-*RR* of the shown RPs. (I)–(III)(F) inter-spike spectrum of the τ-*RR* shown in panels (I)–(III)(E). During the transition from combustion noise to oscillatory instability, the τ-*RR* transforms from wide distribution to a single value, which is reflected in ISS in the form of condensation from a wide spectrum to a dominant mode.

Due to the larger number of longer diagonal lines in periodic states, we observe a higher L compared to the chaotic state.

Diagonal line entropy ($Entr$) measures the variability of the diagonal lines formed from the recurrence points. Here, $p(l) = P(l)/N_l$ is the probability of occurrence of a line of length l, and N_l is the total number of line segments in the RP,[54]

$$Entr = -\sum_{l=l_{\min}}^{N} p(l)\ln p(l). \tag{7}$$

$Entr$ can be interpreted as the averaged measure showing the uncertainty associated with discovering a diagonal line of a specific length (l) within the RP. Consequently, the entropy will be higher for an RP with a broad distribution of diagonal line lengths than for an RP with fewer diagonal line lengths.

2. Measures based on vertical lines

In RPs, a series of recurrence points forming a vertical black line (v) indicates the presence of a trapped part of the trajectory. These vertical black lines are useful for detecting instances where the trajectory evolves very slowly or remains static. Meanwhile, a series of white points in the RP (non-recurrence points) form a vertical white line (k), which can be interpreted as the duration of the non-recurring states or the time interval required for the system to recur; i.e., the recurrence time.

Laminarity (LAM) computes the percentage of recurrence points that form vertical lines (v) longer than $v_{\min}$. Laminarity is analogous to determinism calculated for the diagonal structures in the RP,[55]

$$LAM = \frac{\sum_{v=v_{\min}}^{N} vP(v)}{\sum_{v=1}^{N} vP(v)}. \tag{8}$$

LAM quantifies the occurrence of laminar states in the system. Laminar states correspond to periods of regularity in the behavior of a system, where the system remains in a particular state for an extended period before transitioning to another state.

The trapping time (TT) is the average length of the vertical recurrence lines greater than $v_{\min}$ in the RP. TT provides estimates of the average time the system is trapped in a given state of the dynamical system,[55]

$$TT = \frac{\sum_{v=v_{\min}}^{N} vP(v)}{\sum_{v=v_{\min}}^{N} P(v)}. \tag{9}$$

The recurrence time (RT) is the average empty (white) vertical distance ($k > k_{\min}$) between the recurrence points in an RP. This measure is analogous to the average diagonal line length and the trapping time. The length of the vertical white line between two recurrence points corresponds to the dominant time period during periodic oscillations. Here, the total number of vertical white lines of length k is given by the histogram $P(k)$,[56]

$$RT = \frac{\sum_{k=k_{\min}}^{N} kP(k)}{\sum_{k=k_{\min}}^{N} P(k)}. \tag{10}$$

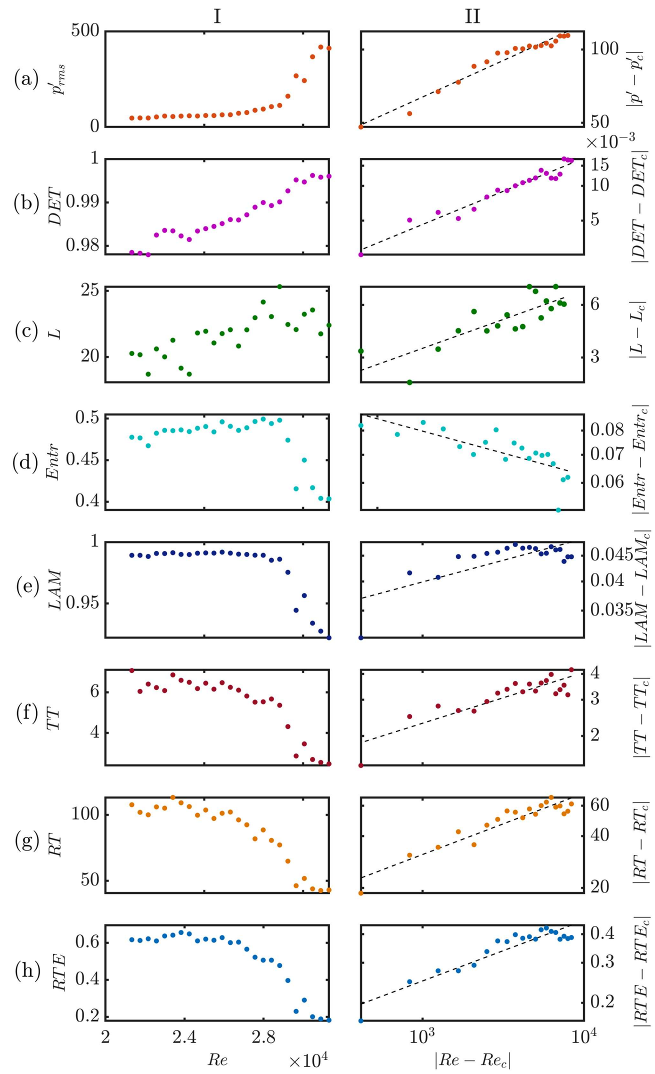

FIG. 3. Scaling of RQA measures with the distance from the critical point. Variation of p'_{rms} I(a) and recurrence measures I(b-h) with control parameter (Re). We observe that all recurrence-based measures anticipate the shift to periodic oscillations in advance. Power-law scaling relations II(a-h) are observed in relation to the corresponding differences in control parameter (Re) and its value at the critical point ($Re_c = 2.96 \pm 0.069 \times 10^4$). We have intermittency at Re_c, which has qualities of both chaos and periodicity.

Recurrence time entropy (RTE) is the Shannon entropy computed for vertical white line structures (k),

$$RTE = -\sum_{k=k_{\min}}^{N} p(k)lnp(k), \tag{11}$$

where $p(k) = P(k)/N_k$ is the probability of occurrence of a line of length k and N_k is the total number of white vertical line segments in the RP.[56] The RTE helps to quantify the uncertainty associated

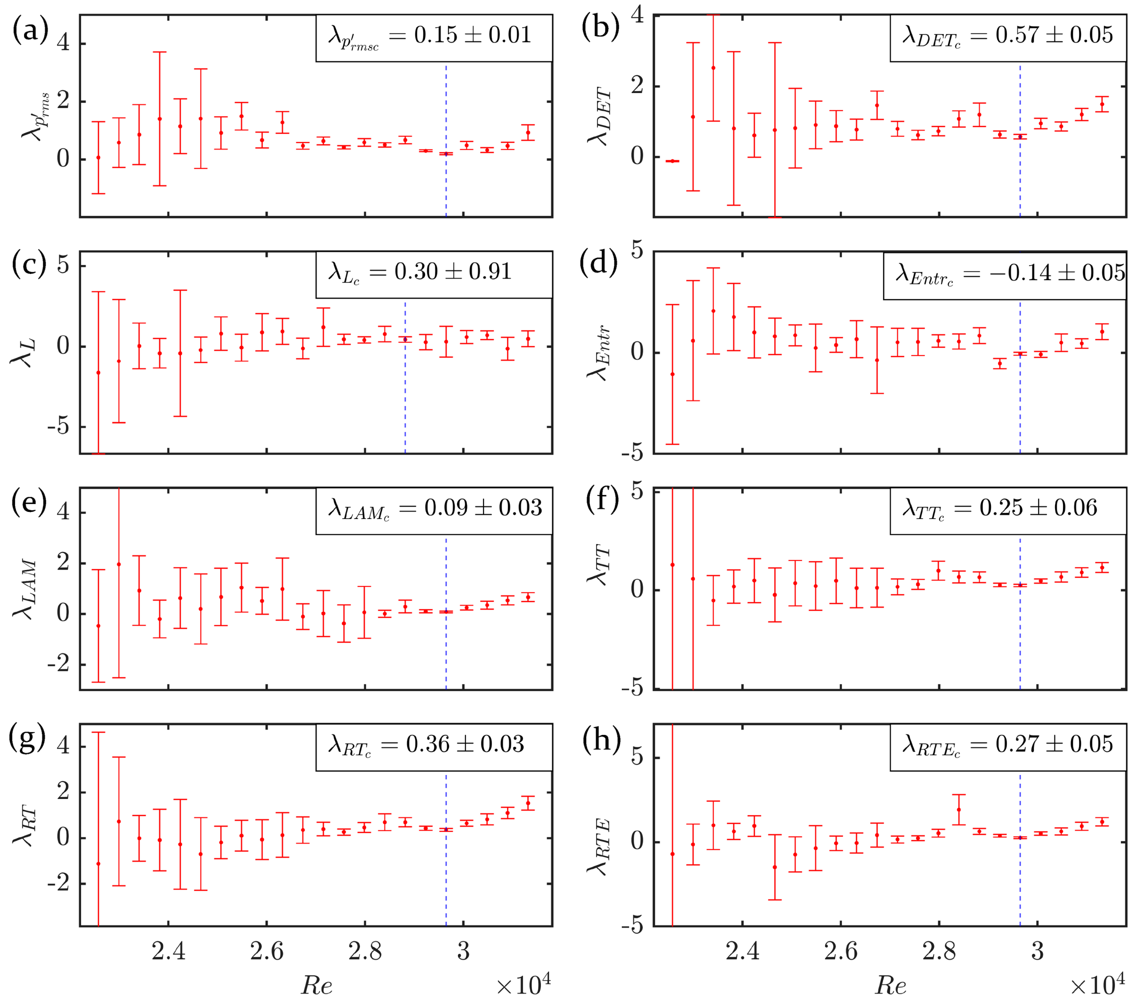

FIG. 4. Scaling exponents and their associated uncertainty. (a-h) The scaling exponent (λ) associated with their corresponding recurrence measures is plotted against the control parameter (*Re*). These error bars indicate the level of uncertainty associated with the corresponding scaling exponent. We observe the minimum uncertainty of the exponent for most of the measures at $Re = (2.96 \pm 0.069) \times 10^4$.

with the recurrence times. During a chaotic state, the time taken to recur to a previously visited neighborhood varies, whereas for the state having periodic oscillations, we observe a constant recurrence time. Thus, the *RTE* for a chaotic state would be higher than that of a periodic state.

III. RESULTS

A. Understanding recurrence condensation

We analyze the data obtained from a thermo-fluid system where different dynamical states were captured by varying the Reynolds number (*Re*) quasi-statically. As *Re* is varied, the system transitions from a state of low-amplitude chaotic fluctuations to a state characterized by high-amplitude self-sustained periodic oscillations via the route of intermittency. Previously, the low-amplitude state of combustion noise has been shown to exhibit high-dimensional deterministic chaos contaminated with colored noise. Tony *et al.*[57] and Nair *et al.*[58] demonstrated the presence of deterministic chaotic behavior and multifractal behavior during combustion noise. The chaotic states observed correspond to statistically stationary asymptotic behavior under fixed control parameters and are not transient responses. The time series of acoustic pressure fluctuations, phase portraits, and their corresponding RPs are shown in Figs. 2(A)–2(D), where the system transitions from combustion noise to thermoacoustic instability. During this critical transition, the patterns in the RPs undergo self-organization, condensing from a wide distribution of time scales represented by the variations in spacing between the diagonal lines (i.e., recurrence times) into a dominant time scale [Fig. 2(D)]. In this system, there is always a dominant peak corresponding to the dominant acoustic mode. The recurrence plots constructed by fixing ε as 20% of the attractor size in the phase space capture the full spectrum of timescales. We can also observe the timescale of bursting as black patches in Fig. 2(I-II)D. The white patches with diagonal structures indicate periodicity within the burst, while the low amplitude chaotic fluctuations appear as black patches. The state of intermittency appears as broken diagonal lines in the RP, capturing the timescale of bursting. Finally, during thermoacoustic instability, we observe long, continuous diagonal lines, indicating the presence of a single dominant timescale.

We capture this condensation using measures quantifying the time scales in the RPs. One such measure is the τ recurrence rate (τ-RR), where we quantify the likelihood of the system recurring after a specific time period. It is essentially the density of the recurrence points along the diagonals of the RPs, measured in τ units from the main diagonal. Consequently, those RPs characterized by long diagonal lines would have a high τ-RR when compared to the broken diagonal lines of varying lengths. This is evident from Fig. 2(E), where we observe the condensation of the τ-RR to a constant value during critical transition. We further decompose the τ-RR using Dirac delta functions to obtain the inter spike spectrum (ISS).[52] The ISS of the τ-RR is akin to the power spectrum, which provides dominant periodicities of the corresponding time series (refer Appendix). The condensation of time scales is also clear in Fig. 2(F), where the ISS transforms from a broad distribution of time periods to a single dominant time period. We define this condensation of time scales in the RPs during the emergence of an order as recurrence condensation.

Although the recurrence plots are constructed using one-dimensional time series (acoustic pressure), the underlying thermoacoustic system is, indeed, a high-dimensional spatiotemporal system.[57–60] In real-world thermoacoustic systems, only acoustic pressure fluctuations can typically be measured, making it a common practice to use the time series of acoustic pressure to study the dynamics, especially in detecting the transition to thermoacoustic instability. The high-dimensional spatiotemporal dynamics and dynamical transitions are reflected in the temporal signals as well. Hence, the recurrence plots capture meaningful information about the high-dimensional dynamics despite being constructed from a single observable.

B. Variation in RQA measures

We quantify recurrence condensation using several recurrence quantification measures. These measures are based on the recurrence point density (RR), diagonal line structures (DET, L, $Entr$), black vertical line structures (LAM, TT), and white vertical line structures (RT, RTE) (refer Methods section for details). To investigate the time-dependent characteristics of a system, we employ a moving window to compute RQA measures.

During the computation of RQA measures, the consideration of minimal line length is important to prevent the inclusion of false recurrences. Here, the minimal diagonal line length ($l_{\min}$), the minimal vertical black line length ($v_{\min}$), and the minimal vertical white line length ($k_{\min}$) are chosen as 2. RQA measures are computed by segmenting the time series into smaller windows of 1500 data points each. For each time series window, RQA measures are individually calculated, and the final RQA values are obtained by averaging these measures across all windows.

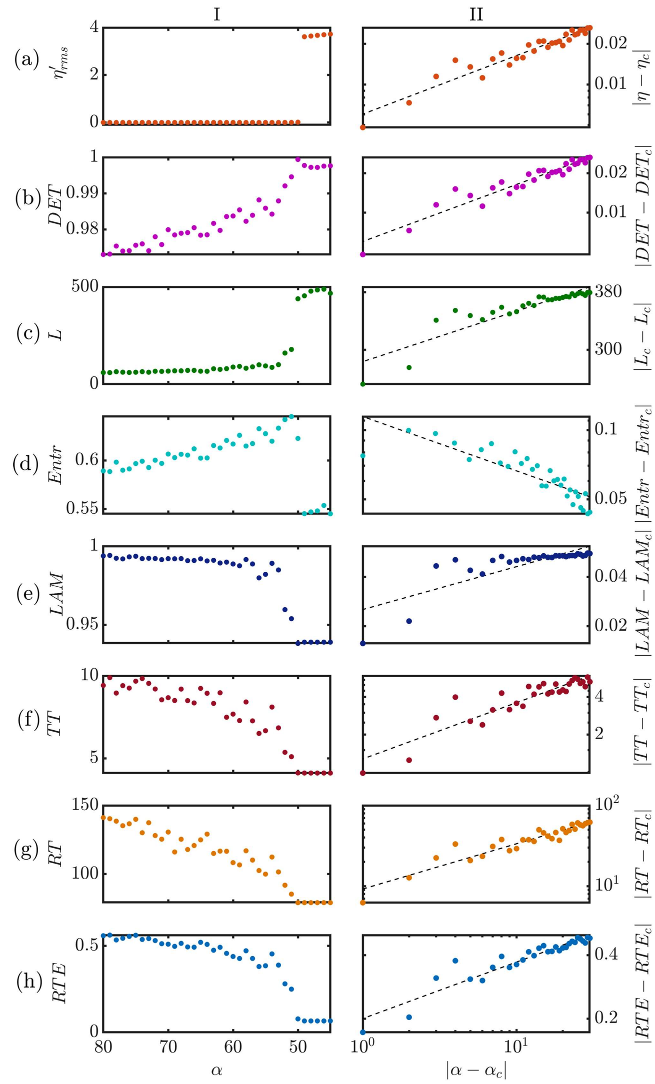

FIG. 5. Scaling of RQA measures for the noisy subcritical Hopf bifurcation. Variation of η'_{rms} I(a) and recurrence measures I(b)–(h) with control parameter (α) and power-law scaling II(a)–(h) with the absolute distance of recurrence measures from its critical point and the absolute distance of control parameter from its value at the critical point (α_c = 50). All these measures calculated up to α_c show power-law scaling. Also, RQA measures such as *DET*, *Entr*, *LAM*, *TT*, *RT*, and *RTE* detect the impending transition to LCO.

Determinism (DET) and average diagonal line length (L) increase as the system transitions to thermoacoustic instability, as observed in Fig. 3(I-b,c). This gradual increase indicates a stronger presence of recurrent patterns characterized by longer diagonal lines in the RPs. The increase in both DET and L suggest a more ordered and predictable behavior in the system. Thus,

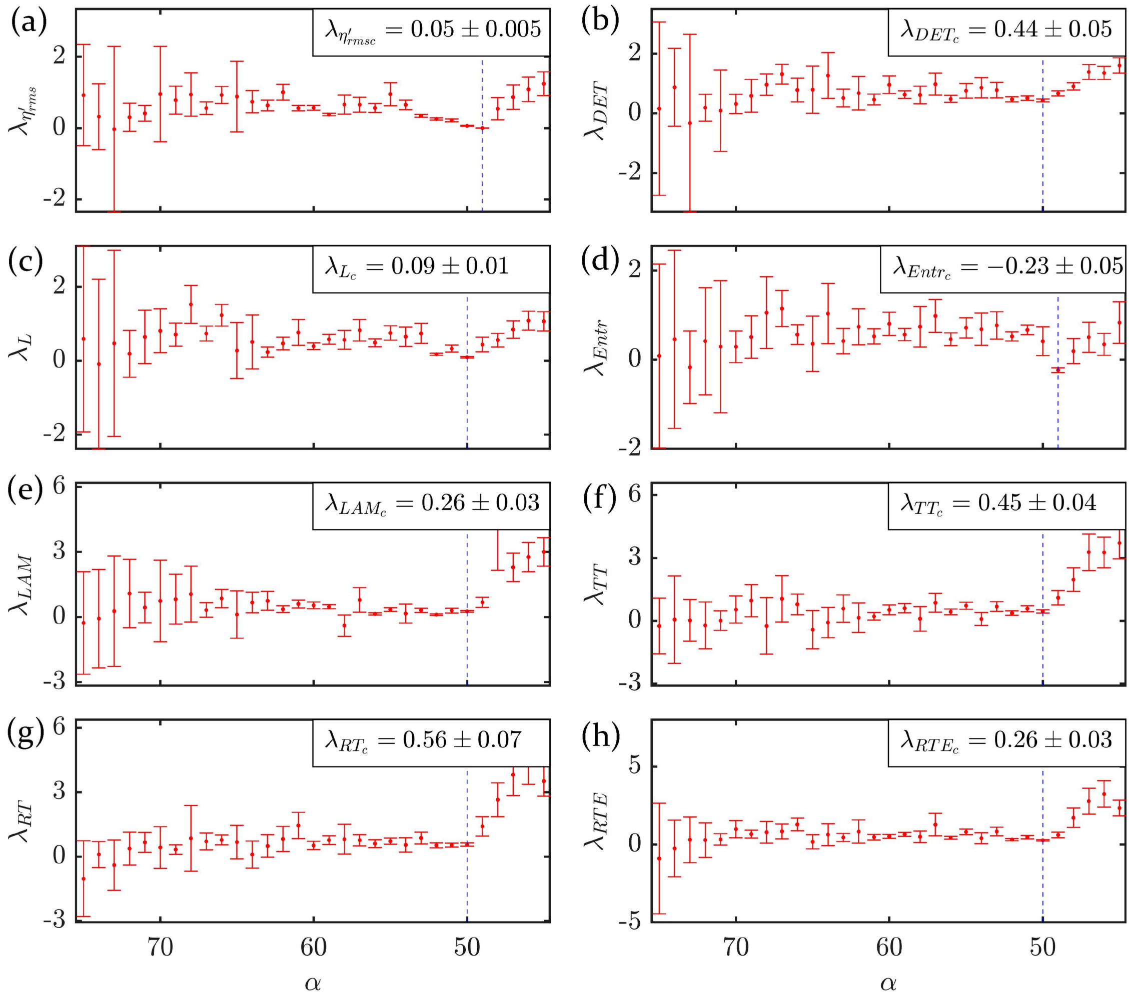

FIG. 6. Scaling exponents and their associated uncertainty for the noisy subcritical Hopf bifurcation model. We observe that the uncertainty of λ is minimal at ($\alpha = 50$) for *DET*, *L*, *LAM*, *TT*, *RT*, and *RTE* (a)–(h). This specific point coincides with the Hopf bifurcation point of the model.

we can characterize self-sustained high-amplitude oscillations, i.e., thermoacoustic instability, as a state of order, while chaotic low-amplitude fluctuations represent a state of disorder.

As shown in Fig. 3(I-d), the diagonal line length entropy (*Entr*) initially increases and then decreases. The initial increase suggests an increase in the complexity of the system. However, as the system approaches thermoacoustic instability, the decrease in entropy implies a reduction in the variability and randomness of the recurrence plot. We further observe that the trapping time (*TT*) and laminarity (*LAM*) decrease [Fig. 3I-(e,f)]. This trend indicates a reduction in the vertical line length, signifying a decrease in the occurrence of trapping states and laminar regions in the RPs. Both recurrence time (*RT*) and recurrence time entropy (*RTE*) show a downward trend [Fig. 3I-(g,h)]. This suggests that as the system approaches thermoacoustic instability, the average time required for a system to recur to a previously visited neighborhood decreases. In summary, we observe that RQA measures such as *DET*, *Entr*, *LAM*, *RT*, and *RTE* detect the impending transition to thermoacoustic instability.

We observe a power-law scaling in the absolute difference between recurrence measures and their values at a certain control parameter value, denoted as Re_c [Fig. 3II(b-h)]. Note that the variations in RQA measures shown in Fig. 3-I are on a linear scale, whereas the power-law scaling in Fig. 3-II are on a log-log scale. This scaling is observed in relation to the corresponding differences in the control parameter (Re) and its critical value (Re_c). For clarity, we refer to this Re_c as the critical point. We calculate this scaling by subtracting the RQA measures calculated at Re_c from the RQA measures determined prior to reaching Re_c. This method is applied iteratively, treating each Re as Re_c. We observe scaling with a good fit for recurrence quantification measures *DET*, *Entr*, *LAM*, *TT*, *RT*, and *RTE* when $Re_c = 2.96 \times 10^4$.

This relationship describes how a RQA measure, denoted as a, behaves according to a power-law pattern with an exponent λ. Mathematically, this power-law relationship can be expressed as $|a - a_c| = |Re - Re_c|^{\lambda}$, where Re_c is the value of the control parameter at a critical point, and a_c is the corresponding RQA measure calculated at Re_c. This equation highlights a scaling behavior in RQA measures calculated before the critical point. As we iteratively vary Re_c, we analyze how the scaling exponent (λ) and its uncertainty for a specific RQA measure varies. We then select the value of Re_c that yields the best power-law fit, as determined by the minimum error between the fitted line and the computed data points. Figure 4 shows λ and its uncertainty as an error bar. The minimum uncertainty in λ is observed at $Re_c = 2.96 \times 10^4$ for measures $p'_{\rm rms}$, *DET*, *Entr*, *LAM*, *TT*, *RT*, and *RTE*. Beyond this critical point, the fitting error increases, indicating a deviation from the power-law scaling behavior. From this, we deduce that the control parameter at which the uncertainty of fitting a power-law is minimum is the critical point for the system. Additionally, the scaling exponents (λ_c) for each RQA measure at the critical point (Re_c) are shown in Figs. 4(a)–4(h).

C. Variation of RQA measures and power-law scaling in mathematical models

To understand the significance of the critical point detected using our method, we construct RPs for the data generated from a model exhibiting noisy subcritical and supercritical Hopf bifurcations (refer Sec. II B). In a supercritical Hopf bifurcation, as the control parameter (α) approaches the Hopf point, the system exhibits a gradual transition from a stable fixed point to a stable limit cycle. Conversely, in a subcritical Hopf bifurcation, the system abruptly jumps from a stable fixed point to an unstable state having large amplitude limit cycle oscillations. To understand the different dynamical states in these transitions, we compute and quantify the RPs using RQA measures and capture the evolution of RQA measures as the control parameter (α) varies.

1. Subcritical Hopf bifurcation

The recurrence quantification measures change with the change in the value of the control parameter and shift abruptly at the Hopf point ($\alpha = 50$). We observe an abrupt jump in $\eta'_{\rm rms}$ from a state of fixed point to a state of LCO [Fig. 5(I-a)]. However, we see notable variations in RQA measures such as *DET*, *L*, *Entr*, *LAM*, *TT*, *RT*, and *RTE* before the system reaches limit cycle oscillations [Fig. 5I(b)–(h)]. The observed variations in the recurrence measures align with the previously discussed trend for a thermofluid system transitioning toward thermoacoustic instability [Fig. 3I(b-h)]. We also find a similar power-law scaling of the absolute difference between recurrence measures computed before reaching the critical control parameter value (α_c) with the RQA measures at α_c [Fig. 5I(b-h)]. This scaling is observed with the corresponding differences in the control parameters α and α_c. To determine the best-fit line, we calculate the uncertainty of the scaling exponent λ. This involves assessing the uncertainty associated with the value of λ at various values of the control parameter. We find that the uncertainty of λ is minimal at $\alpha_c = 50$. This implies that all RQA measures calculated up to the Hopf point of the system, i.e., $\alpha = 50$, show a power-law scaling with the corresponding difference in α and α_c. The uncertainties of λ for various RQA measures are shown in Figs. 6(a)–6(h). Therefore, we reveal that the critical point identified via this method is, indeed, the Hopf bifurcation point of the model.

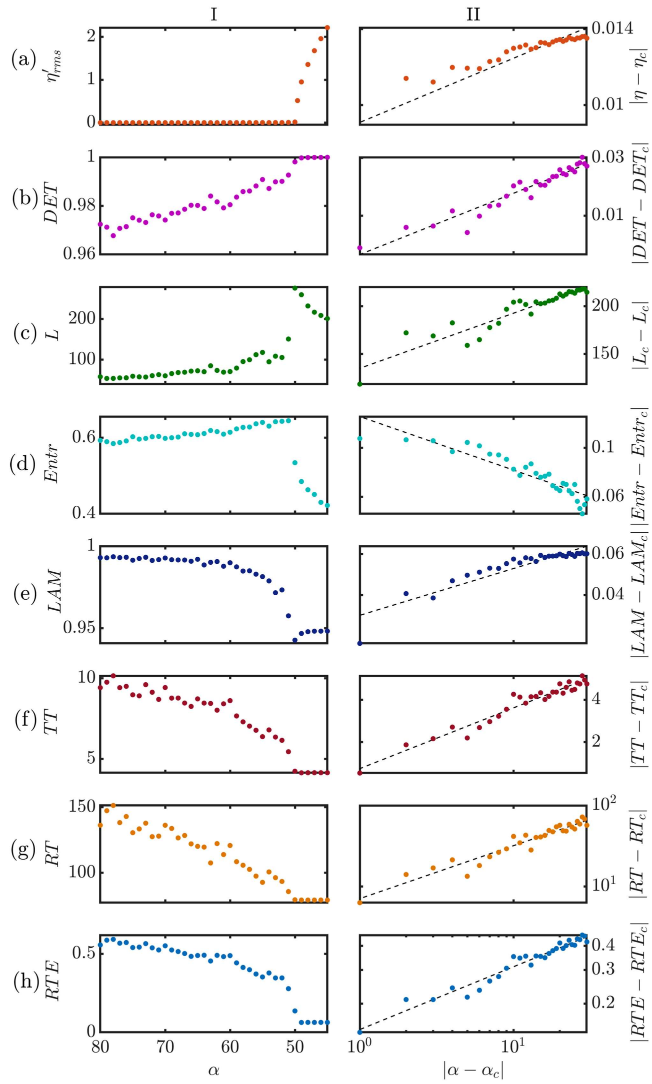

FIG. 7. Scaling of RQA measures for the noisy supercritical Hopf bifurcation. The variation of $\eta'_{\rm rms}$ I (a) and recurrence measures I (b)–(h) with control parameter (α) and power-law scaling II (a)–(h) at the critical point α_c of the system are shown. The best-fit line is obtained by considering all RQA measures up to $\alpha_c = 50$.

2. Supercritical Hopf bifurcation

We perform RQA for the supercritical Hopf bifurcation, where we observe a gradual transition from a fixed point to a state characterized by limit cycle oscillations. This transition is evident from the variation in $\eta_{\rm rms}$, which changes from a low value in the steady state

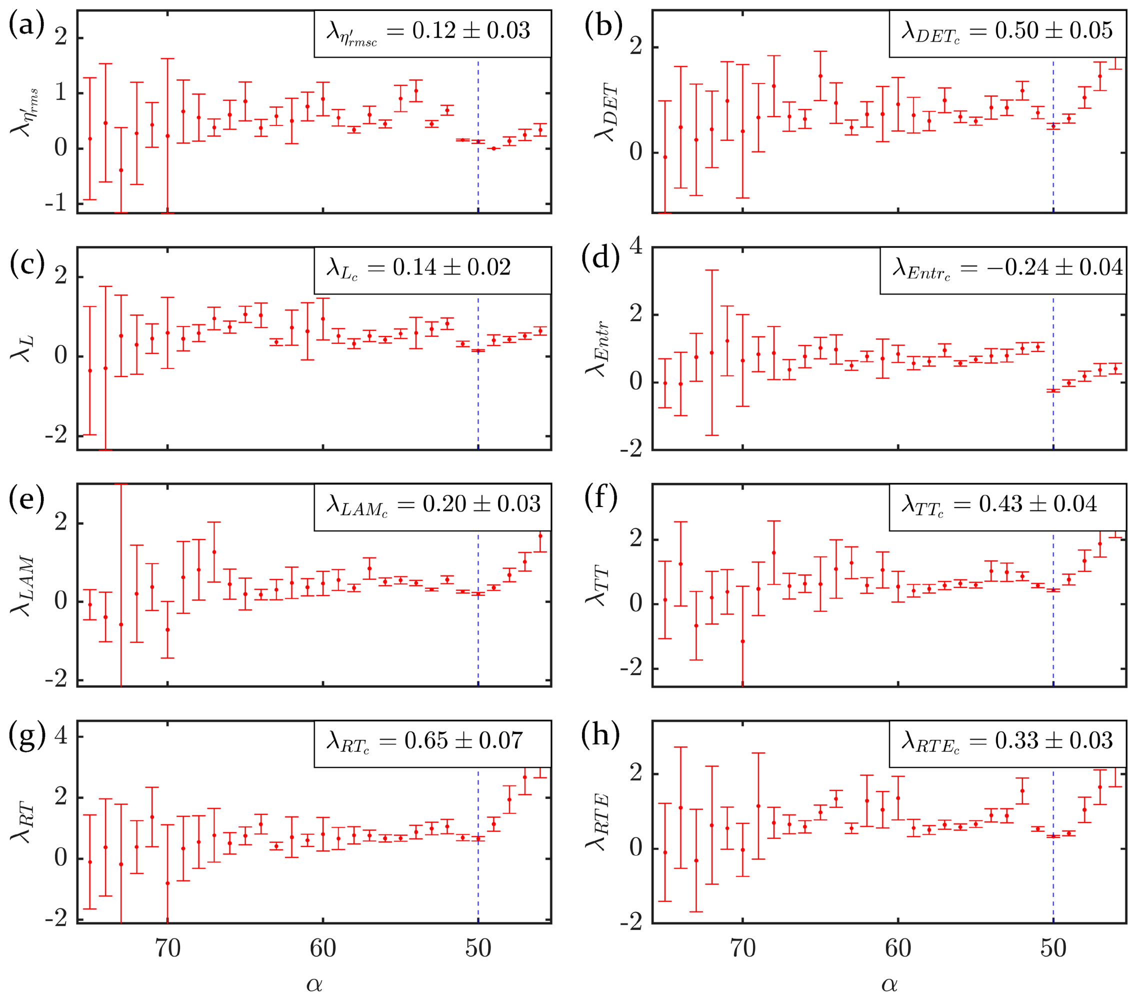

FIG. 8. Scaling exponents and their associated uncertainty for the noisy supercritical Hopf bifurcation model. Measures $\eta_{\rm rms}$, *DET*, *L*, *Entr*, *LAM*, *TT*, *RT*, and *RTE* show a minimum error bar at $\alpha_c = 50$ (a-h). This signifies that the critical point is detected by considering the point at which the deviation from the fitted line is minimum. The best-fit line is obtained by considering all RQA measures up to the Hopf point of the system.

to a higher value in the LCO regime, reflecting the growth in oscillation amplitude [Fig. 7(I-a)]. Here, the Hopf point is at a control parameter value of $\alpha = 50$, and periodic oscillations are observed at $\alpha = 49$. The variations in RQA measures align with the previously discussed trends in the thermo-fluid system [Fig. 3I(b)–(h)] and the subcritical Hopf bifurcation model [Fig. 5I(b)–(h)]. By leveraging the scale-invariant property of the system at its critical point, we find a power-law scaling of the RQA measures [Fig. 7II(b-h)]. The measures $\eta_{\rm rms}$, *DET*, *L*, *LAM*, *TT*, *RT*, and *RTE* show minimum uncertainty in λ at $\alpha_c = 50$ [Fig. 8(a)–(h)]. This implies that all RQA measures calculated up to the Hopf point of the system, i.e., $\alpha = 50$, exhibit a power-law scaling with the corresponding difference in α and α_c. The variation of scaling exponents, calculated for all the recurrence measures is illustrated in Fig. 9. These power-law exponents from the thermoacoustic system, the subcritical Hopf bifurcation model, and the supercritical Hopf bifurcation model are plotted in the same figure, for comparison. The exponents appear to be different for each system, although their values are close. The purpose of introducing theoretical models is not to replicate the experimental system in full, but to show that recurrence-based methods can effectively detect such transitions and identify the critical points. To this end, we used a basic normal form of the Hopf bifurcation, to interpret the results in comparison with a standard model.

Our method serves as a reliable technique for identifying the critical point of a system with broader applications across various transitions. By calculating the RQA measures, we show that these measures can help in characterizing various dynamical states observed in a critical transition. Additionally, power-law scaling relations are observed with the deviation of RQA measures from

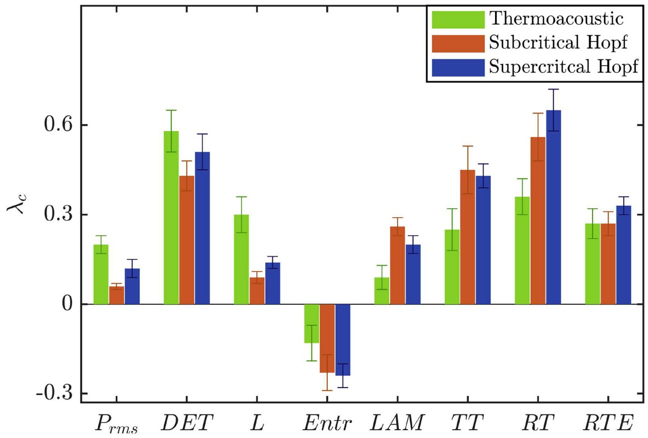

FIG. 9. Variation in λ_c of RQA measures across the thermoacoustic system, as well as the subcritical and supercritical Hopf bifurcation models. Here, the scaling exponent values for RQA measures are observed to differ across the systems.

the critical point with the distance to the critical point. The critical point detected through our method is the same as the Hopf point. This confirms the effectiveness of our approach in pinpointing the critical transition point.

IV. DISCUSSIONS AND CONCLUSION

Studying complex systems is crucial for understanding similarities across diverse fields, including ecology, finance, climate science, and biology. These systems exhibit multi-stability, leading to critical transitions where even small perturbations can induce abrupt shifts from one state to another, with significant consequences. Thermo-fluid systems, such as thermoacoustic, aeroacoustic, and aeroelastic systems, often transition from small-amplitude aperiodic fluctuations to high-amplitude oscillatory instabilities, posing serious threats to their structural integrity and functionality. One of the intriguing aspects of complex systems is the phenomenon of self-organization, where coherent, ordered patterns emerge from the initially disordered states as observed in various physical and biological systems. These instances highlight the ability of complex systems to organize themselves into coherent structures spontaneously.

We investigate the phenomena of "recurrence condensation" observed in RPs during the critical transitions in turbulent thermoacoustic systems. This phenomenon, analogous to spectral condensation, involves the convergence of multiple recurrence time scales into a single dominant time scale during the transition from combustion noise to thermoacoustic instability.

Through the application of RQA, we identify the critical transition points and observe certain RQA measures exhibiting power-law scaling behavior. In our work, the scaling exponents for these power laws are calculated based on the distance between the recurrence measures evaluated prior to a critical point. In a study by Afsar *et al.*,[44] a similar power-law scaling was observed for recurrence measures during the transition from period-doubling to chaos. In contrast, our system undergoes a transition from low-amplitude chaotic behavior to large amplitude periodic oscillations. Despite these differences in transition pathways, both studies reveal a power-law behavior in the recurrence measures. This highlights the universal nature of scaling laws in capturing the underlying dynamical changes, even across different types of transitions. Interestingly, while the scaling exponents of the RQA measures differ, most RQA measures accurately identify the critical point. In the case of Hopf bifurcation models, this critical point corresponds to the Hopf bifurcation point. This finding underscores the potential of RQA as a valuable tool for detecting the critical transitions in noisy turbulent systems, particularly in fluid dynamics, where precise pinpointing of the transition points is challenging.

Our approach to use RPs and their quantification within reactive flow systems offers a promising method for identifying critical points with broad applicability across diverse fields. Through a careful selection of thresholds and parameters, our method provides a robust framework for detecting critical points during a transition.

ACKNOWLEDGMENTS

R.I.S. acknowledges the Department of Science and Technology, Government of India for providing the funding from IoE initiative (No. SP22231222CPETWOCTSHOC) and SERB/CRG/2020/003051.

AUTHOR DECLARATIONS

Conflict of Interest

The authors have no conflicts to disclose.

Author Contributions

Manaswini Jella: Conceptualization (supporting); Formal analysis (equal); Investigation (equal); Methodology (equal); Software (equal); Validation (lead); Visualization (lead); Writing – original draft (lead); Writing – review & editing (equal). **Induja Pavithran:** Conceptualization (equal); Formal analysis (equal); Investigation (equal); Methodology (equal); Software (equal); Validation (equal); Writing – original draft (equal); Writing – review & editing (equal). **Vishnu R. Unni:** Conceptualization (equal); Data curation (lead); Formal analysis (supporting); Investigation (equal); Methodology (equal); Project administration (supporting); Supervision (supporting); Validation (equal); Writing – review & editing (equal). **Norbert Marwan:** Conceptualization (lead); Investigation (supporting); Methodology (equal); Software (equal); Supervision (equal); Validation (equal); Writing – review & editing (equal). **Jürgen Kurths:** Formal analysis (supporting); Investigation (supporting); Methodology (equal); Project administration (equal); Supervision (equal); Validation (equal); Writing – review & editing (equal). **R. I. Sujith:** Conceptualization (equal); Data curation (supporting); Formal analysis (supporting); Funding acquisition (lead); Investigation (equal); Project administration (lead); Resources (equal); Supervision (lead); Writing – review & editing (equal).

DATA AVAILABILITY

The data that support the findings of this study are available from the corresponding author upon reasonable request.

APPENDIX: CALCULATION OF INTER-SPIKE SPECTRUM ON τ-RR

As defined in Sec. II D, the τ-RR of an RP refers to the recurrence rate along a diagonal line, measured at a distance of τ units perpendicular to the main diagonal of the recurrence matrix. Often the τ-RR of the RPs show a spike-train like structure. Due to this nature, the interpretation from its Fourier transform is challenging. Thus, instead of decomposing the τ-RR based on trigonometric basis functions, ISS is generated using Dirac delta combs.[52] These Dirac combs are generated by introducing the Dirac delta function at different inter-spike periods (T_{is}) resulting in a series of vertical spikes. For a signal (s) of length N, T_{is} has an upper bound of $M = N/2 + 1$. This upper bound is useful in removing redundant or ambiguous periods, thus generating a set of linearly independent basis functions. Here, let χ be the set of basis functions generated using Dirac combs. In order to generate s from χ ($M \times N$ matrix), we need to solve the under-determined linear system as shown in Eq. (A1).

$$\chi^T \beta = s. \tag{A1}$$

Here, β is the loadings of each individual basis function. For a clear interpretation of dominant periodicities present in the signal, sparsity in β is required. In this paper, the least absolute shrinkage and selection operator (LASSO) regularization technique[52] is used to solve β. The regularization threshold is carefully selected to ensure that the Pearson correlation coefficient (ρ) between the obtained signal and the reconstructed signal using χ highlights the dominant periodicities. In this case, we set ρ to 0.9 to identify significant correlations.

REFERENCES

[1] S. H. Strogatz, "Exploring complex networks," Nature **410**, 268–276 (2001).
[2] Y. Bar-Yam, "General features of complex systems," in *Encyclopedia of Life Support Systems (EOLSS)* (UNESCO Publishers, Oxford, 2002).
[3] J. F. Donges, R. V. Donner, N. Marwan, S. F. Breitenbach, K. Rehfeld, and J. Kurths, "Non-linear regime shifts in Holocene Asian monsoon variability: Potential impacts on cultural change and migratory patterns," Clim. Past **11**, 709–741 (2015).
[4] M. Small, *Applied Nonlinear Time Series Analysis: Applications in Physics, Physiology and Finance* (World Scientific Publishing, Singapore, 2005).
[5] R. N. Mantegna and H. E. Stanley, *Introduction to Econophysics: Correlations and Complexity in Finance* (Cambridge University Press, 1999).
[6] T. M. Lenton, H. Held, E. Kriegler, J. W. Hall, W. Lucht, S. Rahmstorf, and H. J. Schellnhuber, "Tipping elements in the Earth's climate system," Proc. Natl. Acad. Sci. U.S.A. **105**, 1786–1793 (2008).
[7] N. Marwan, N. Wessel, U. Meyerfeldt, A. Schirdewan, and J. Kurths, "Recurrence-plot-based measures of complexity and their application to heart-rate-variability data," Phys. Rev. E **66**, 026702 (2002).
[8] S. Kelso, *Dynamic Patterns: The Self-Organization of Brain and Behavior* (MIT Press, 1995).
[9] M. Scheffer, *Critical Transitions in Nature and Society* (Princeton University Press, 2009).
[10] M. Scheffer and S. R. Carpenter, "Catastrophic regime shifts in ecosystems: Linking theory to observation," Trends Ecol. Evol. **18**, 648–656 (2003).
[11] N. Marwan, J. F. Donges, R. V. Donner, and D. Eroglu, "Nonlinear time series analysis of palaeoclimate proxy records," Quat. Sci. Rev. **274**, 107245 (2021).
[12] J. Jhun, P. Palacios, and J. O. Weatherall, "Market crashes as critical phenomena? Explanation, idealization, and universality in econophysics," Synthese **195**, 4477–4505 (2018).
[13] S. Mariappan and R. I. Sujith, "Thermoacoustic instability in a solid rocket motor: Non-normality and nonlinear instabilities," J. Fluid Mech. **653**, 1–33 (2010).
[14] V. Godavarthi, V. Unni, E. Gopalakrishnan, and R. I. Sujith, "Recurrence networks to study dynamical transitions in a turbulent combustor," Chaos **27**, 063113 (2017).
[15] J. M. Drake, T. S. Brett, S. Chen, B. I. Epureanu, M. J. Ferrari, E. Marty, P. B. Miller, E. B. O'dea, S. M. O'regan, A. W. Park *et al.*, "The statistics of epidemic transitions," PLoS Comput. Biol. **15**, e1006917 (2019).
[16] I. Pavithran, V. R. Unni, A. J. Varghese, R. I. Sujith, A. Saha, N. Marwan, and J. Kurths, "Universality in the emergence of oscillatory instabilities in turbulent flows," EPL **129**, 24004 (2020).
[17] A. Hirschberg, X. Pelorson, and J. Gilbert, "Aeroacoustics of musical instruments," Meccanica **31**, 131–141 (1996).
[18] G. Flandro and J. Majdalani, "Aeroacoustic instability in rockets," AIAA J **41**, 485–497 (2003).
[19] R. I. Sujith and S. A. Pawar, *Thermoacoustic Instability: A Complex Systems Perspective* (Springer International Publishing, 2021).
[20] S. Fisher and S. Rahman, *Remembering the Giants: Apollo Rocket Propulsion Development*, Monographs in Aerospace History (NASA History Division, Office of External Relations, 2009).
[21] M. C. Cross and P. C. Hohenberg, "Pattern formation outside of equilibrium," Rev. Mod. Phys. **65**, 851–1112 (1993).
[22] Z. Wu, "The self-organization phenomenon in Rayleigh-Benard convection: A hydrodynamics analysis," arXiv:1011.4443 [physics.flu-dyn] (2010).
[23] H. Haken, "Synergetics: An introduction nonequilibrium phase transitions and self-organization in physics, chemistry and biology," Phys. Bull. **28**, 412 (1977).
[24] R. C. Desai and R. Kapral, "Turing patterns," in *Dynamics of Self-Organized and Self-Assembled Structures* (Cambridge University Press, 2009), pp. 201–211.
[25] K. B. Davis, M.-O. Mewes, M. R. Andrews, N. J. van Druten, D. S. Durfee, D. Kurn, and W. Ketterle, "Bose–Einstein condensation in a gas of sodium atoms," Phys. Rev. Lett. **75**, 3969 (1995).
[26] A. Chiocchetta, A. Gambassi, I. Carusotto *et al.*, "Laser operation and Bose–Einstein condensation: Analogies and differences," in *Universal Themes of Bose-Einstein Condensation* (Cambridge University Press, 2017), pp. 409–423.
[27] S. Tandon and R. I. Sujith, "Condensation in the phase space and network topology during transition from chaos to order in turbulent thermoacoustic systems," Chaos **31**, 043126 (2021).
[28] J. Buck and E. Buck, "Synchronous fireflies," Sci. Am. **234**, 74–85 (1976).
[29] W. Friesen and G. Block, "What is a biological oscillator?" Am. J. Physiol. Regul. Integr. Comp. Physiol. **246**, R847–R853 (1984).
[30] W. Wang, I. Z. Kiss, and J. L. Hudson, "Experiments on arrays of globally coupled chaotic electrochemical oscillators: Synchronization and clustering," Chaos **10**, 248–256 (2000).
[31] I. Kiss and J. Hudson, "Chemical complexity: Spontaneous and engineered structures," AIChE J. **49**, 2234–2241 (2003).
[32] I. Pavithran, V. R. Unni, A. J. Varghese, D. Premraj, R. I. Sujith, C. Vijayan, A. Saha, N. Marwan, and J. Kurths, "Universality in spectral condensation," Sci. Rep. **10**, 17405 (2020).
[33] N. Marwan, "A historical review of recurrence plots," Eur. Phys. J.: Spec. Top. **164**, 3–12 (2008).
[34] L. Trulla, A. Giuliani, J. Zbilut, and C. Webber, "Recurrence quantification analysis of the logistic equation with transients," Phys. Lett. A **223**, 255–260 (1996).
[35] N. Marwan, M. C. Romano, M. Thiel, and J. Kurths, "Recurrence plots for the analysis of complex systems," Phys. Rep. **438**, 237–329 (2007).
[36] E. J. Ngamga, D. V. Senthilkumar, A. Prasad, P. Parmananda, N. Marwan, and J. Kurths, "Distinguishing dynamics using recurrence-time statistics," Phys. Rev. E **85**, 026217 (2012).
[37] N. Boers, J. Kurths, and N. Marwan, "Complex systems approaches for earth system data analysis," J. Phys.: Complex. **2**, 011001 (2021).
[38] E. Gopalakrishnan, Y. Sharma, T. John, P. Dutta, and R. I. Sujith, "Early warning signals for critical transitions in a thermoacoustic system," Sci. Rep. **6**, 35310 (2016).

[39] S. V. George, S. Kachhara, R. Misra, and G. Ambika, "Early warning signals indicate a critical transition in betelgeuse," Astron. Astrophys. **640**, L21 (2020).
[40] V. Nair and R. I. Sujith, "Multifractality in combustion noise: Predicting an impending combustion instability," J. Fluid Mech. **747**, 635–655 (2014).
[41] L. Kabiraj and R. I. Sujith, "Nonlinear self-excited thermoacoustic oscillations: Intermittency and flame blowout," J. Fluid Mech. **713**, 376–397 (2012).
[42] V. Nair, G. Thampi, and R. I. Sujith, "Intermittency route to thermoacoustic instability in turbulent combustors," J. Fluid Mech. **756**, 470–487 (2014).
[43] B. I. Halperin and P. C. Hohenberg, "Scaling laws for dynamic critical phenomena," Phys. Rev. **177**, 952–971 (1969).
[44] O. Afsar, D. Eroglu, N. Marwan, and J. Kurths, "Scaling behaviour for recurrence-based measures at the edge of chaos," EPL **112**, 10005 (2015).
[45] C. Wilke, "A viscosity equation for gas mixtures," J. Chem. Phys. **18**, 517–519 (1950).
[46] N. Noiray, "Linear growth rate estimation from dynamics and statistics of acoustic signal envelope in turbulent combustors," J. Eng. Gas Turbines Power **139**, 041503 (2017).
[47] J.-P. Eckmann, O. Oliffson Kamphorst, and D. Ruelle, "Recurrence plots of dynamical systems," EPL **4**, 973–977 (1987).
[48] L. Cao, "Practical method for determining the minimum embedding dimension of a scalar time series," Physica D **110**, 43–50 (1997).
[49] A. M. Fraser and H. L. Swinney, "Independent coordinates for strange attractors from mutual information," Phys. Rev. A **33**, 1134–1140 (1986).
[50] N. Marwan, M. Carmen Romano, M. Thiel, and J. Kurths, "Recurrence plots for the analysis of complex systems," Phys. Rep. **438**, 237–329 (2007).
[51] K. H. Kraemer, R. V. Donner, J. Heitzig, and N. Marwan, "Recurrence threshold selection for obtaining robust recurrence characteristics in different embedding dimensions," Chaos **28**, 085720 (2018).
[52] K. H. Kraemer, F. Hellmann, M. Anvari, J. Kurths, and N. Marwan, "Spike spectra for recurrences," Entropy **24**, 1689 (2022).
[53] S. Schinkel, N. Marwan, O. Dimigen, and J. Kurths, "Confidence bounds of recurrence-based complexity measures," Phys. Lett. A **373**, 2245–2250 (2009).
[54] D. Eroglu, T. K. D. Peron, N. Marwan, F. A. Rodrigues, L. D. F. Costa, M. Sebek, I. Z. Kiss, and J. Kurths, "Entropy of weighted recurrence plots," Phys. Rev. E **90**, 042919 (2014).
[55] N. Marwan, M. C. Romano, M. Thiel, and J. Kurths, "Recurrence plots for the analysis of complex systems," Phys. Rep. **438**, 237–329 (2007).
[56] M. R. Sales, M. Mugnaine, J. D. Szezech, R. L. Viana, I. L. Caldas, N. Marwan, and J. Kurths, "Stickiness and recurrence plots: An entropy-based approach," Chaos **33**, 033140 (2023).
[57] J. Tony, E. A. Gopalakrishnan, E. Sreelekha, and R. I. Sujith, "Detecting deterministic nature of pressure measurements from a turbulent combustor," Phys. Rev. E **92**, 062902 (2015).
[58] V. Nair, G. Thampi, S. Karuppusamy, S. Gopalan, and R. I. Sujith, "Loss of chaos in combustion noise as a precursor of impending combustion instability," Int. J. Spray Combust. Dyn. **5**, 273–290 (2013).
[59] Y. Okuno, M. Small, and H. Gotoda, "Dynamics of self-excited thermoacoustic instability in a combustion system: Pseudo-periodic and high-dimensional nature," Chaos **25**, 043107 (2015).
[60] V. Godavarthi, V. Unni, E. Gopalakrishnan, and R. I. Sujith, "Recurrence networks to study dynamical transitions in a turbulent combustor," Chaos **27**, 063113 (2017).